Geochemical proxies of North American freshwater routing during the Younger Dryas cold event

Anders E. Carlson*†, Peter U. Clark*, Brian A. Haley‡, Gary P. Klinkhammer§, Kathleen Simmons¶, Edward J. Brook*, and Katrin J. Meissner‖

*Department of Geosciences, Oregon State University, Corvallis, OR 97331; ‡The Leibniz Institute of Marine Sciences, University of Kiel, D-24148 Kiel, Germany; §College of Oceanic and Atmospheric Sciences, Oregon State University, Corvallis, OR 97331; ¶U.S. Geological Survey, Denver, CO 80225; and ‖School of Earth and Ocean Sciences, University of Victoria, Victoria, BC, Canada V8W 3P6

Edited by James P. Kennett, University of California, Santa Barbara, CA, and approved February 27, 2007 (received for review December 19, 2006)

The Younger Dryas cold interval represents a time when much of the Northern Hemisphere cooled from ≈12.9 to 11.5 kiloyears B.P. The cause of this event, which has long been viewed as the canonical example of abrupt climate change, was initially attributed to the routing of freshwater to the St. Lawrence River with an attendant reduction in Atlantic meridional overturning circulation. However, this mechanism has recently been questioned because current proxies and dating techniques have been unable to confirm that eastward routing with an increase in freshwater flux occurred during the Younger Dryas. Here we use new geochemical proxies (ΔMg/Ca, U/Ca, and $^{87}Sr/^{86}Sr$) measured in planktonic foraminifera at the mouth of the St. Lawrence estuary as tracers of freshwater sources to further evaluate this question. Our proxies, combined with planktonic $\delta^{18}O_{seawater}$ and $\delta^{13}C$, confirm that routing of runoff from western Canada to the St. Lawrence River occurred at the start of the Younger Dryas, with an attendant increase in freshwater flux of 0.06 ± 0.02 Sverdrup (1 Sverdrup = 10^6 $m^3 \cdot s^{-1}$). This base discharge increase is sufficient to have reduced Atlantic meridional overturning circulation and caused the Younger Dryas cold interval. In addition, our data indicate subsequent fluctuations in the freshwater flux to the St. Lawrence River of ≈0.06–0.12 Sverdrup, thus explaining the variability in the overturning circulation and climate during the Younger Dryas.

abrupt climate change | Atlantic meridional overturning circulation | paleoclimate

Proxies of deepwater formation show that a large reduction in the Atlantic meridional overturning circulation (AMOC) occurred at the start of the Younger Dryas event (1–3), suggesting that the attendant loss of ocean heat transport caused Younger Dryas cooling in the North Atlantic region. However, the cause of this ocean response remains unclear, with the leading mechanism, involving the routing of continental runoff to the St. Lawrence River (4–8), now questioned on the basis of marine (9–11) and terrestrial (12, 13) evidence and modeling (14). Moreover, the rate of the AMOC varied during the Younger Dryas (1–3), which is not readily explained by the conventional routing argument (4–8). This debate has led to the questioning of the role of freshwater in forcing abrupt climate change (13), with important implications to our understanding of the sensitivity of the AMOC to global warming and attendant changes in the hydrological cycle.

Here we capitalize on the well known relation between river geochemistry and underlying bedrock lithology (15) to use changes in $^{87}Sr/^{86}Sr$, U/Ca, and Mg/Ca measured in planktonic foraminifera tests as tracers of routing of continental runoff derived from distinct geological terranes. The conventional argument for the cause of the Younger Dryas (4–8) invokes the opening of the eastern Lake Agassiz outlet and the Straits of Mackinaw ≈12,900 calibrated years B.P. (all dates reported here are in calibrated radiocarbon years unless otherwise specified) by retreat of the southern Laurentide Ice Sheet margin, effectively doubling the size of the St. Lawrence River drainage basin, from 1.35×10^6 km^2 to 3.13×10^6 km^2 (7) (Fig. 1). Because the newly added drainage area included significantly different bedrock lithologies than those underlying the St. Lawrence drainage area before this event (16) (Fig. 1), the associated routing of surface water should thus be marked by changes in St. Lawrence water geochemistry (15). To assess geochemical changes associated with these new sources of surface water, we picked planktonic foraminifera from two cores in the outer St. Lawrence estuary (Fig. 1) that span the Younger Dryas interval: *Globigerina bulloides* and *Neogloboquadrina pachyderma* (s) from core HU90031-047 (45°51.14′N, 57°37.56′W; 473-m depth) and *G. bulloides* from core HU90031-044 (44°39.41′N, 55°37.13′W; 1,381-m depth).

Results

Changes in Mg/Ca, U/Ca, and $^{87}Sr/^{86}Sr$ identify changes in the source and flux of surface waters reaching the St. Lawrence estuary during the Younger Dryas (Fig. 2). Mean Mg/Ca values in *G. bulloides* from core 044 range from 1.1 to 3 mmol/mol (Fig. 2*d*). Changes in Mg/Ca in foraminifera reflect temperature- and salinity-dependent uptake of Mg as well as changes in the [Mg] and [Ca] of the water (17, 18). We use an existing sea surface temperature (SST) record from core 044, based on dinoflagellate–cyst assemblages (11) (Fig. 2*a*), to account for SST changes in our Mg/Ca record by applying the *G. bulloides* calibration {Mg/Ca (mmol/mol) = $0.474\exp[0.107 \times \text{SST}(°\text{C})]$} (18). The persistence of sea ice in the St. Lawrence estuary for 9 months of the year during the Younger Dryas (11) indicates that planktonic foraminifera grew in the 3 months of summer, the season of the SST reconstruction. We then estimate salinity variations in the estuary on the basis of a $\delta^{18}O_{seawater}$ record from core 044 (Fig. 2*b*), and we applied a salinity calibration [Mg/Ca (mmol/mol) = $0.311 \times$ salinity] (18). These combined corrections have a propagated error of ≈30% (16) [see supporting information (SI) *Methods*]. Subtracting these temperature and salinity components from our measured Mg/Ca values and normalizing to the lowest resulting value produces a ΔMg/Ca record that reflects changes in Mg/Ca of the estuary.

Foraminiferal ΔMg/Ca increases by ≈2.5 mmol/mol at the onset of the Younger Dryas (Fig. 2*d*), a signal that had been masked in our Mg/Ca record by the corresponding decrease in

Author contributions: A.E.C. and P.U.C. designed research; A.E.C., B.A.H., G.P.K., and K.S. performed research; A.E.C., B.A.H., G.P.K., and K.S. contributed new reagents/analytic tools; A.E.C., P.U.C., E.J.B., and K.J.M. analyzed data; and A.E.C. and P.U.C. wrote the paper.

The authors declare no conflict of interest.

This article is a PNAS Direct Submission.

Abbreviations: Sv, Sverdrup; AMOC, Atlantic meridional overturning circulation; SST, sea surface temperature; kyr BP, kiloyears B.P.

See Commentary on page 6500.

†To whom correspondence should be sent at the present address: Department of Geology and Geophysics, Woods Hole Oceanographic Institution, Woods Hole, MA 02543. E-mail: acarlson@whoi.edu.

This article contains supporting information online at www.pnas.org/cgi/content/full/0611313104/DC1.

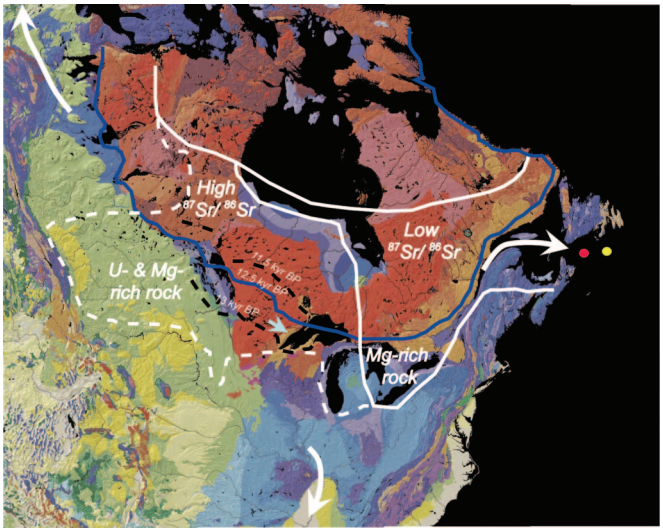

Fig. 1. Bedrock map of central–eastern North America (16) showing major lithologies that influence river geochemistry. Colors are coded according to bedrock age: red shades are Precambrian, blue shades are Paleozoic, green shades are Mesozoic, and yellow is Cenozoic. We have identified those geochemical properties of bedrock types that produce distinctive signals in drainage basins. The western part of the Canadian Precambrian Shield has higher $^{87}Sr/^{86}Sr$ than the eastern Shield, Paleozoic sedimentary bedrock underlying the eastern Great Lakes includes Mg-rich dolomite, and Mesozoic sedimentary bedrock of the western Canadian Plains is enriched in U and Mg. Also shown is the outline (in blue) of the 12.5 calibrated kyr B.P. ice margin (26) and the southwestern margin of the Laurentide Ice Sheet at the start of the Younger Dryas (13 calibrated kyr B.P.) and near the end of the Younger Dryas (11.5 calibrated kyr B.P.) (26) (dashed black lines) [the age of these margins, however, is not constrained by dates (26)]. The solid white line is the pre-Younger Dryas drainage area of the St. Lawrence River with its northern margin controlled by the ice sheet divide (7). The dashed white line represents the additional area routed to the St. Lawrence River at the start of the Younger Dryas (7). White arrows indicate the freshwater drainage routes to the Arctic, the Gulf of Mexico, and the St. Lawrence River, and the blue arrow indicates the general location of the eastern outlet for glacial Lake Agassiz. Core locations in the outer St. Lawrence estuary are shown as a red dot (core 90031-047) and a yellow dot (core 90031-044).

SST and salinity (Fig. 2 *a* and *b*). We attribute this increase to the routing of western Canadian runoff to the St. Lawrence River due to retreat of ice out of the Lake Superior Basin. Specifically, rivers draining shale and carbonate bedrock in areas of western Canadian Plains that were routed to the St. Lawrence basin during the Younger Dryas (Fig. 1) have [Mg] that are ≈6–10 times higher (≈0.6–1.0 mmol/kg) than the [Mg] of the integrated St. Lawrence River system (≈0.1 mmol/kg) (19) before the Younger Dryas. At ≈12.7 kiloyears B.P. (kyr B.P.), ΔMg/Ca increases again by ≈1.5 mmol/mol, indicating a further increase in freshwater flux from western Canadian Plains.

Using our geochemical mixing model and assuming similar river chemistry as today and a pre-Younger Dryas flux of 0.07 Sverdrup (Sv) (7) (1 Sv = 10^6 $m^3 \cdot s^{-1}$), we find that an increase of 0.07 Sv in freshwater discharge for the St. Lawrence River (Fig. 3) derived from these source waters would explain the initial Younger Dryas ΔMg/Ca signal (see *SI Methods*). The subsequent increase in ΔMg/Ca at 12.7 kyr B.P. can be explained by an additional flux increase of 0.06 Sv (Fig. 3). Because the dinoflagellate–cyst SST reconstruction records temperature near the water surface whereas *G. bulloides* may live deeper in the mixed layer, the increases in ΔMg/Ca and modeled base flow discharge during the Younger Dryas are maximum estimates. However, evidence for atmospheric cooling in Maritime Canada (20) and mixed-layer cooling in the shelf water of the North Atlantic adjacent to the St. Lawrence

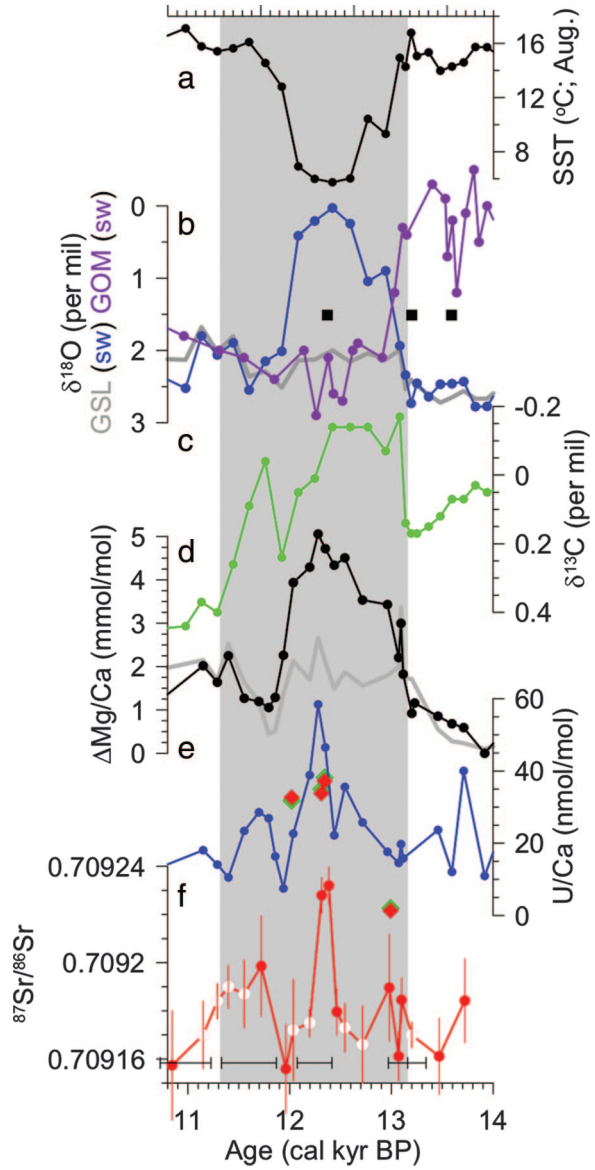

Fig. 2. Geochemical time series (in calibrated radiocarbon kyr B.P.) for the Younger Dryas interval. (*a*) Dinoflagellate cyst SST reconstruction (HU90031-044) (9). (*b*) Planktonic [*N. pachyderma* (s)] $\delta^{18}O$ (gray) (11) and of seawater (blue) for the St. Lawrence (SL) (HU90031-044); and planktonic (*Globigerinoides ruber*) $\delta^{18}O_{seawater}$ record from the Gulf of Mexico (GOM) (purple) (31). Black squares denote the reported calibrated age control (31). (*c*) Planktonic [*N. pachyderma* (s)] $\delta^{13}C$ record (green) from the St. Lawrence (HU90031-044) (courtesy of C. Hillaire-Marcel). (*d*) Mg/Ca (gray) and ΔMg/Ca (black) of *G. bulloides* (HU90031-044). (*e*) U/Ca of *G. bulloides* (blue from HU90031-044 and green from HU90031-047) and *N. pachyderma* (s) (red from HU90031-047). The offset in U/Ca between 044 and 047 before the Younger Dryas reflects the different proximity of the cores to the riverine end-member. (*f*) Sr isotopes of *G. bulloides* (HU90031-044). White symbols with red outline represent thermal ionization MS measurements; red symbols with white outline represent multicollector inductively coupled plasma MS measurements. The gray bar denotes the time of eastward routing as inferred from our geochemical proxies of routing. Horizontal bars at the bottom indicate calibrated radiocarbon age control for core HU90031-044.

estuary (10) provides strong support for substantial cooling of the St. Lawrence estuary during the Younger Dryas and the temperature correction.

Foraminiferal U/Ca in *G. bulloides* and *N. pachyderma* (s) from core 047 and in *G. bulloides* from core 044 all reach peak values that

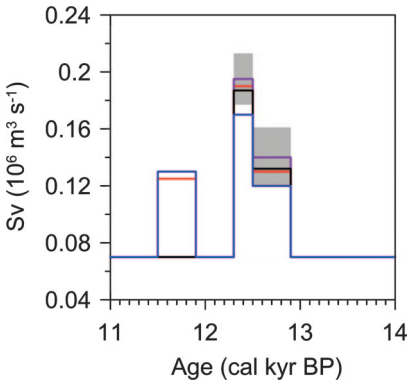

Fig. 3. Time series (in calibrated radiocarbon kyr B.P.) of modeled freshwater discharge from the St. Lawrence River. The model is initiated with a flux of 0.07 Sv (7) and then solved to match the routing data (see *SI Methods*). $^{87}Sr/^{86}Sr$ is in red, U/Ca is in blue, $\delta^{18}O_{seawater}$ is in black, and ΔMg/Ca is in purple, with gray denoting the ≈30% propagated error (see *SI Methods*).

are ≈30–35 nmol/mol higher in Younger Dryas samples relative to older samples (Fig. 2*e*). The primary sources of seawater U are from U dissolved in rivers, by colloid and particulate disintegration at high salinities (practical salinity units >20) (21), and by release from marine sediments in response to an increase in bottom-water oxygen, such as may be associated with an increased flux of oxygenated freshwater into the St. Lawrence estuary during a routing event. Assuming reasonable values for [U] (25 ppm) in sediment with a 1-m sediment mixed-layer depth distributed over the area of the estuary, a change from anoxic to oxic conditions would release 24×10^6 moles of U to the estuary, corresponding to a foraminiferal U/Ca signal of ≈0.7 nmol/mol (22), or significantly less than our measured values. On the other hand, rivers draining shale and carbonate bedrock of the western Canadian Plains (Fig. 1) have average [U] values (10–20 nmol/kg) that are 10–20 times greater than the [U] of the integrated St. Lawrence River system (23) before the Younger Dryas. Our measured increase in U/Ca is thus consistent with the routing of U-rich surface waters from the western Canadian Plains after the opening of the eastern outlet of Lake Agassiz.

Unlike the ΔMg/Ca record, however, the initial U/Ca increase is gradual until 12.7 kyr B.P., when it rapidly rises to a peak at 12.5 kyr B.P. We attribute the slow initial rise in U/Ca to the offsetting effect of $[CO_3^{-2}]$ on U/Ca in foraminifera tests, such that a doubling to tripling of $[CO_3^{-2}]$ discharged into the estuary due to the increased area draining carbonate terranes would reduce the U/Ca in foraminifera tests by ≈4 nmol/mol (24). Moreover, U release from colloid and particulate disintegration at high salinities will increase exponentially with river flux (see *SI Methods*). By including the carbonate ion effect and the breakdown of colloids and particulates, our mixing model of estuary geochemistry indicates that an increase in discharge through the St. Lawrence River of 0.05 Sv at the start of the Younger Dryas would explain the ≈10 nmol/mol increase in foraminiferal U/Ca, with an additional flux increase of 0.05 Sv at 12.7 kyr B.P. explaining the subsequent peak U/Ca values (Fig. 3) (see *SI Methods*).

Foraminiferal $^{87}Sr/^{86}Sr$ show little change at the start of the Younger Dryas, followed by a rapid increase in $^{87}Sr/^{86}Sr$ at 12.5 kyr B.P. that is 7×10^{-5} higher than $^{87}Sr/^{86}Sr$ in samples that predate the Younger Dryas (Fig. 2*f*). Global seawater $^{87}Sr/^{86}Sr$ is invariant on this timescale, whereas river $^{87}Sr/^{86}Sr$ varies as a function of bedrock age and the duration of chemical weathering of granitoid sediment (25), suggesting that these fluctuations reflect changes in the $^{87}Sr/^{86}Sr$ and flux of runoff to the St. Lawrence River. At the time of initial opening of the eastern Lake Agassiz outlet, exposed western Canadian Precambrian Shield had been deglaciated for at least 1,000 years (26), so that $^{87}Sr/^{86}Sr$ of granitoid sediment would be comparable to modern bedrock values (0.72450) (25). Our mixing model (see *SI Methods*) indicates that an initial flux increase of 0.06 Sv at the start of the Younger Dryas (Fig. 3) (as suggested by ΔMg/Ca and U/Ca) with higher $^{87}Sr/^{86}Sr$ associated with older bedrock of the western Canadian Shield than the younger bedrock of the eastern Canadian Shield (0.71423) (27) would cause foraminiferal $^{87}Sr/^{86}Sr$ to increase by 1×10^{-5}, which is within the uncertainty of our measurements in the early Younger Dryas samples. Subsequent retreat of the southwestern LIS margin (26) (Fig. 1), which was likely enhanced by atmospheric feedbacks associated with the enlarging area of Lake Agassiz (28), exposed Precambrian Shield bedrock, thus spiking runoff with high $^{87}Sr/^{86}Sr$ (0.79500) due to the release of radiogenic Sr from young granitoid soils (25). Assuming initial $^{87}Sr/^{86}Sr$ similar to modern values in surface waters of Canada (27), we find that a subsequent increase in freshwater flux of 0.06 Sv (Fig. 3) combined with radiogenic Sr derived from weathering of freshly exposed granitoid sediment after ice retreat explains the abrupt increase in $^{87}Sr/^{86}Sr$ at 12.5 kyr B.P. (see *SI Methods*).

Discussion

Our multiproxy approach addresses the fact that, for any given proxy, additional factors (e.g., temperature and weathering) modulate the signal of changes in freshwater flux. In doing so, we find a clear signal of routing of surface waters from western Canada to the St. Lawrence River at the start of the Younger Dryas, as originally proposed by Johnson and McClure (4). In particular, our three geochemical tracers of source waters independently converge in indicating that freshwater discharge through the St. Lawrence River increased by 0.06 ± 0.02 Sv (average of our three estimates with 2σ error) at the start of the Younger Dryas with a subsequent increase of 0.06 ± 0.01 Sv during the Younger Dryas for a total flux increase of 0.12 ± 0.02 Sv. Our estimate of the initial flux increase (0.06 ± 0.02 Sv) is in good agreement with a previously estimated flux of ≈0.07 Sv (7). The total freshwater flux increase of 0.12 ± 0.02 Sv would decrease estuarine mixed-layer salinity by 4.1 ± 0.6 practical salinity units.

The planktonic $\delta^{13}C$ record in core 044 provides additional support for substantial changes in freshwater flux to the Gulf of St. Lawrence during the Younger Dryas. The $\delta^{13}C$ of dissolved inorganic carbon in freshwater primarily reflects some combination of the $\delta^{13}C$ of soil CO_2 derived from decay of organic matter (lighter values) and the $\delta^{13}C$ of any underlying carbonate bedrock (heavier values). We attribute the abrupt 0.32 per mil decrease in $\delta^{13}C$ (the only anomaly in the 14.5-kiloyear record; reproducibility < 0.05 per mil) at the start of the Younger Dryas (Fig. 2*c*) to indicate an increased flux of ^{12}C-enriched surface runoff reflecting the routing of freshwater from the western Canadian Plains to the St. Lawrence. However, $\delta^{13}C$ does not show any change at a time (12.7 to 12.5 kyr B.P.) when ΔMg/Ca, U/Ca, and $^{87}Sr/^{86}Sr$ suggest an increase in freshwater flux. This lack of a signal may reflect a larger contribution from ^{12}C-depleted bedrock relative to soil CO_2, thus offsetting any change in $\delta^{13}C$ associated with an increased freshwater flux.

These combined results appear contrary to the modest 0.5 per mil decrease in $\delta^{18}O_{calcite}$ measured in *N. pachyderma* (s) from core 044 (Fig. 2*b*), which deVernal *et al.* (11) used along with salinity reconstructions based on dinoflagellate–cysts to argue against any significant salinity decrease in the St. Lawrence estuary during the Younger Dryas. However, $\delta^{18}O_{calcite}$ reflects the combination of the offsetting effects of temperature and salinity, so that a 10°C decrease in SSTs during the Younger Dryas at this site (11) (Fig. 2*a*) would mask an additional 2.25 per mil salinity signal in $\delta^{18}O_{calcite}$, corresponding to a net 2.75 per mil decrease in $\delta^{18}O_{seawater}$ (Fig. 2*b*). Similar to the ΔMg/Ca record, this total 2.75 per mil $\delta^{18}O_{seawater}$ decrease is a maximum estimate due to the depth–habitat difference between the dinoflagellates (the SST source) and *N. pachy-*

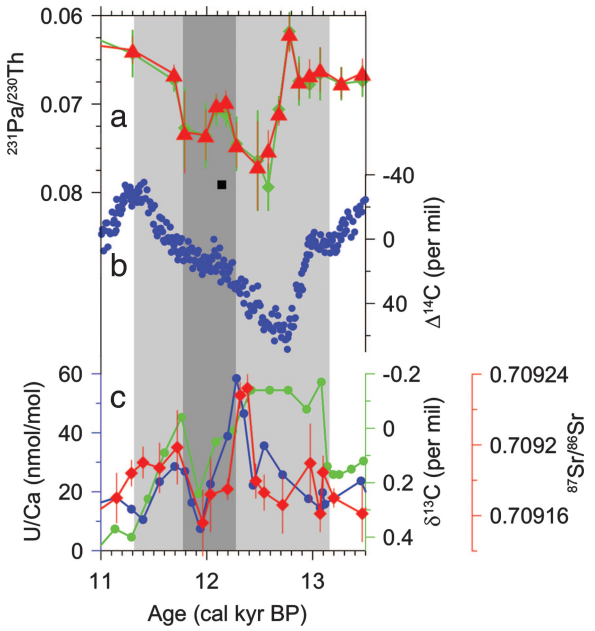

Fig. 4. Proxies of AMOC and freshwater routing. (*a*) $^{231}Pa/^{230}Th$ record from the subtropical North Atlantic (red diamonds are the ^{232}Th method, and green diamonds are the ^{238}U method) (2). Age control is indicated by the black square. (*b*) Detrended $\Delta^{14}C$ from Cariaco Basin (1). (*c*) Planktonic U/Ca (blue), $\delta^{13}C$ (green), and $^{87}Sr/^{86}Sr$ (red) from HU90031-044. The vertical light gray bar denotes the timing of the Younger Dryas as inferred from our geochemical proxies of routing, and the vertical dark gray bar denotes the intra-Younger Dryas event defined by our geochemical routing proxies.

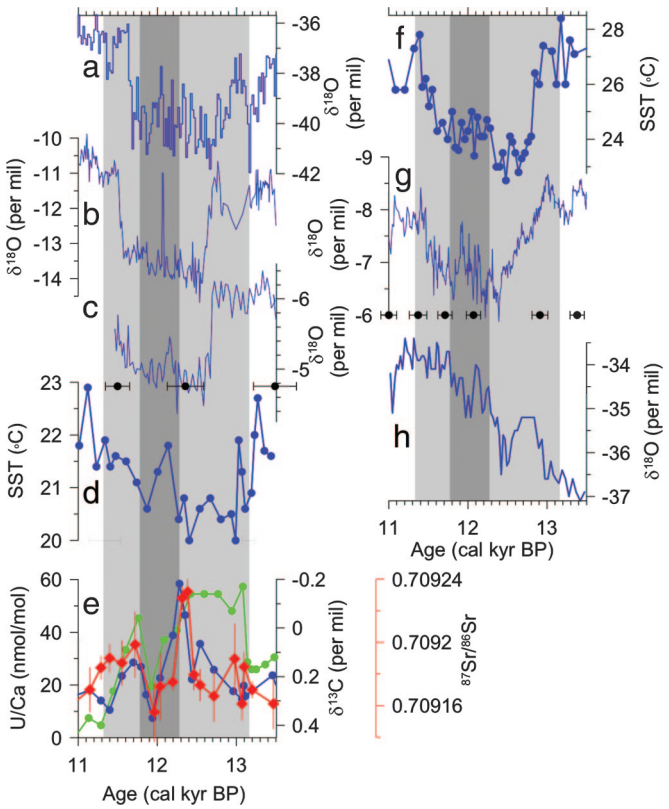

Fig. 5. Proxies of climate change and freshwater routing during the Younger Dryas. (*a*) Greenland $\delta^{18}O$ record (38). (*b*) $\delta^{18}O$ from Ammerssee Lake, Germany (40). (*c*) $\delta^{18}O$ from Chauvet Cave, France (39). Black symbols with error bars denote age control. (*d*) SST reconstruction from the coast of West Africa (36). Horizontal bars denote calibrated radiocarbon age control. (*e*) Planktonic U/Ca (blue), $\delta^{13}C$ (green), and $^{87}Sr/^{86}Sr$ from HU90031-044. (*f*) SST reconstruction from Cariaco Basin (37). (*g*) $\delta^{18}O$ from Hulu Cave, China (41). Black symbols with error bars denote age control. (*h*) $\delta^{18}O$ record from Byrd ice core, Antarctic (42). Vertical gray bars are the same as in Fig. 4.

derma (s). However, a freshwater flux increase of 0.11 Sv (Fig. 3) derived from western Canadian source waters with $\delta^{18}O$ of −25 per mil (29) would have decreased estuarine mixed-layer $\delta^{18}O$ by 2.75 per mil (see *SI Methods*). This flux increase is in good agreement with the estimated increase (0.12 ± 0.02 Sv) from our three routing proxies, thus supporting the temperature correction in core 044.

We note that the stacked $\delta^{18}O_{calcite}$ record measured on *N. pachyderma* (s) from the continental margin off Nova Scotia also shows an ≈0.8 per mil decrease during the Younger Dryas (10) (SI Fig. 6 *a* and *b*), which, if corrected for Younger Dryas cooling suggested by the large increase in percentage of *N. pachyderma* (s) from the same cores (SI Fig. 6*c*), would approach the $\delta^{18}O_{seawater}$ change suggested from St. Lawrence estuary (see *SI Methods* and SI Fig. 6*b*). In addition, open ocean $\delta^{18}O_{calcite}$ records measured on *G. bulloides* and *N. pachyderma* (s) from Orphan Knoll show a 1–1.25 per mil decrease during the Younger Dryas (30), which would be closer to the $\delta^{18}O_{seawater}$ change in the St. Lawrence estuary if the temperature decrease was taken into account. The salinity decrease in the St. Lawrence is also contemporaneous with a 2.5–2.75 per mil increase in $\delta^{18}O_{seawater}$ from the Orca Basin, Gulf of Mexico (31) (Fig. 2*b*), thus supporting Johnson and McClure's hypothesis (4) that routing of North American runoff from the Mississippi River to the St. Lawrence River occurred at the start of the Younger Dryas. Although the dinoflagellate–cyst salinity reconstruction of de Vernal *et al.* (11) lacks a freshening signal, the combined evidence from our $^{87}Sr/^{86}Sr$, U/Ca, and ΔMg/Ca records as well as the planktonic $\delta^{13}C$ and $\delta^{18}O_{seawater}$ records all indicating reduced salinity suggest that the dinoflagellate–cyst salinity reconstruction for the St. Lawrence estuary is in error during the Younger Dryas.

According to the conventional routing hypothesis, surface waters from western Canada continued to drain through the eastern outlet of Lake Agassiz to the St. Lawrence River until ≈11.5 kyr B.P., when ice readvance across the outlet rerouted surface waters either to the south (Mississippi River) (6–8) or to the northwest (Mackenzie River) (32) (Fig. 1). In contrast, all proxies from core 044 indicate that salinity started to increase ≈12.3–12.4 kyr B.P. and reached pre-Younger Dryas values by ≈12 kyr B.P. (Fig. 2), implying a decrease to pre-Younger Dryas freshwater discharge (Fig. 3) and suggesting that rerouting occurred earlier. The terrestrial record of routing during this time period is poorly constrained, but two lines of evidence suggest that this previously unrecognized intra-Younger Dryas routing event occurred through the northwestern Clearwater Outlet to the Arctic Ocean via the Mackenzie River (Fig. 1): a radiocarbon age of 10,310 ± 290 ^{14}C yr B.P. (12,040 ± 400 calibrated years B.P.) on a piece of wood obtained in flood deposits from the outlet (32) with two additional supporting radiocarbon dates on wood of the same age (33), and a light planktonic $\delta^{18}O$ anomaly in a record from the Beaufort Sea that dates at 12 kyr B.P. (34) using the most recent reservoir age for this region (26).

Three proxies from core 044 (U/Ca, $^{87}Sr/^{86}Sr$, and $\delta^{13}C$) indicate that freshwater flux to the St. Lawrence River subsequently increased for the remainder of the Younger Dryas, whereas $\delta^{18}O_{seawater}$ and ΔMg/Ca show no change (Fig. 2). We attribute the increase in $^{87}Sr/^{86}Sr$, U/Ca, and $\delta^{13}C$ to renewed routing of western Canadian runoff to the St. Lawrence, possibly due to isostatic uplift of the northwest outlet to the Arctic Ocean, causing Lake Agassiz waters to again start draining to the east. Based on our geochemical modeling, this subsequent rerouting would have increased the flux out of the St. Lawrence River by 0.06 ± 0.01 Sv (Fig. 3) (see *SI*

Table 1. Radiocarbon ages obtained from cores 047 and 044

Core	Depth, cm	Material	Sample ID	^{14}C age*	Calibrated age range
90031-044	20.3	*N. pachyderma* (s)	TO-4004	2,610 ± 70	2,150–2,320
90031-044	40	*N. pachyderma* (s)	TO-4005	4,230 ± 70	4,150–4,300
90031-044	140	*N. pachyderma* (s)	TO-4006	10,040 ± 200	10,570–10,880
90031-044	180	*N. pachyderma* (s)	TO-4007	10,500 ± 170	11,290–11,750
90031-044	220	*N. pachyderma* (s)	TO-4008	10,840 ± 90	11,940–12,370
90031-044†	267	Shell	AA-57317	11,520 ± 150	12,870–13,170
90031-044	300	*N. pachyderma* (s)	TO-4409	11,890 ± 100	13,150–13,420
90031-044	410	*N. pachyderma* (s)	TO-4606	12,890 ± 190	14,700–15,218
90031-044	550	*N. pachyderma* (s)	TO-4607	12,950 ± 110	14,740–15,250
90031-047†‡	426	Shell	CAMS-102060	11,020 ± 120	12,510–12,750
90031-047†	444	Shell	CAMS-102059	10,810 ± 45	12,170–12,490
90031-047†	496	Shell	CAMS-102061	11,520 ± 310	12,300–13,850

Data include new ages from this study and previously published radiocarbon ages from core 044 (11). Calibrated ages are reservoir-corrected (11, 26) and calibrated (44) with 1σ error.
*Not reservoir-corrected.
†New dates from this study.
‡Date excluded from the age model.

Methods). The absence of an equivalent ΔMg/Ca signal at this time may in part reflect source-rock changes in the eastern Great Lakes region, whereby the opening of more northerly outlets allowed westerly derived waters from the Agassiz basin to bypass Lakes Erie and Ontario and flow directly from Lake Huron into the St. Lawrence River by way of the Ottawa River (9, 26). The attendant loss of Mg-rich waters due to bypassing the dolomites of the Erie and Ontario basins (Fig. 1) would thus have counteracted the gain of Mg-rich waters derived from the Agassiz basin. However, we should expect to see an ≈2.5–4 mmol/mol gain in ΔMg/Ca relative to a loss of ≈1 mmol/mol due to bypassing carbonate bedrock of the eastern Great Lakes. The absence of a ΔMg/Ca signal as well as a $\delta^{18}O_{seawater}$ signal during this late Younger Dryas time may thus result from the ≈30% error in the ΔMg/Ca record (see *SI Methods*) due to the temperature and salinity adjustments (18) and the ≈20% error in the SST reconstruction (11) with its propagated effect on $\delta^{18}O_{seawater}$.

Our source-water tracers thus provide the first direct oceanographic evidence of eastward routing of surface waters from western Canada to the St. Lawrence River at the start of the Younger Dryas. According to climate models, our estimated freshwater flux increase (0.06 ± 0.02 Sv initially, 0.12 ± 0.02 Sv maximum) required to produce measured changes in $^{87}Sr/^{86}Sr$, U/Ca, ΔMg/Ca, and $\delta^{18}O_{seawater}$ would be sufficient to induce a significant reduction in the AMOC (35), such as occurred during the Younger Dryas (1–3) (Fig. 4). Our results thus resolve the timing of continental routing during this critical period of deglaciation and suggest that the increase in base flow discharge in the St. Lawrence River forced the Younger Dryas cold event. Our results also offer strategies for investigating whether similar mechanisms may have been responsible for other abrupt climate changes.

In addition, our source-water tracers reveal the cause of ocean and climate variability that occurred during the Younger Dryas. All our routing proxies show that, rather than a constant flux of freshwater as generally implied by the conventional routing mechanism (7, 8), freshwater base discharge varied during the Younger Dryas with a two-stepped increase at the start of the Younger Dryas followed by a decrease to pre-Younger Dryas values centered at ≈12 kyr B.P. when freshwater was diverted to the Arctic Ocean. This intra-Younger Dryas routing event is in excellent agreement with proxies that indicate an increase in the AMOC (1–3) (Fig. 4) and attendant warming of the surface ocean (36, 37) (Fig. 5 *d* and *f*) and atmosphere (38–40) (Fig. 5 *a–c*), increased southeast Asian monsoon intensity (41) (Fig. 5*g*), and a cooling over Antarctica (42) (Fig. 5*h*) during the Younger Dryas. These same proxies then suggest that the AMOC subsequently decreased (Fig. 4) with an attendant climate response at a time when our tracers suggest a rerouting of western Canadian freshwater back to the St. Lawrence River (Fig. 5). This tight coupling between changes in freshwater fluxes to the North Atlantic basin, changes in the AMOC, and changes in climate further emphasizes the sensitivity of the climate system to relatively small changes in the hydrological cycle.

Methods

Samples were physically cleaned, prepared with a flow-through method that removes any effects of diagenesis and overgrowths (43), and analyzed by high-resolution inductively coupled plasma MS for U/Ca and Mg/Ca. Sr isotopes were analyzed by multicollector inductively coupled plasma MS and thermal ionization MS. We constructed age models from previously published ^{14}C ages for 044 (11) and new ^{14}C dates from 044 and 047 (Table 1), giving us age control approximately every 430 years (Fig. 2). All ^{14}C ages are reservoir-corrected (11, 26) and calibrated (44). The agreement between benthic mollusk shell ages and planktonic foraminifera ages (11) indicates that any changes in the freshwater flux to the estuary did not affect the reservoir age.

We thank A. deVernal and C. Hillaire-Marcel (GEOTOP, Montreal, QC, Canada) for isotope data; the Bedford Institute of Oceanography (Dartmouth, NS, Canada) for samples; L. Keigwin (Woods Hole Oceanographic Institution) for foraminifera count and isotope data; the Saskatchewan Watershed Authority for river chemistry data; A. Unger for assistance with flow-through processing; M. Cheseby and J. Padman for assistance with foraminifera picking; and D. Barber, G. Clarke, S. Hostetler, A. Mix, and D. Muhs for helpful comments and discussion. Comments and suggestions from two anonymous reviewers greatly improved this article. This research was funded by the National Science Foundation Paleoclimate Program (P.U.C.) and the National Science Foundation (G.P.K.).

1. Hughen KA, Southon JR, Lehman SJ, Overpeck JT (2000) *Science* 290:1951–1954.
2. McManus JF, Francois R, Gherard J-M, Keigwin LD, Brown-Leger S (2004) *Nature* 428:834–837.
3. Eltgroth SF, Adkins JF, Robinson LF, Southon J, Kashgarian M (2006) *Paleoceanography* 21:PA4207.
4. Johnson RG, McClure BT (1976) *Quaternary Res* 6:325–353.
5. Rooth C (1982) *Prog Oceanogr* 11:131–149.
6. Broecker WS, Kennett JP, Flower BP, Teller JT, Trumbore S, Bonani G, Wolffi W (1989) *Nature* 341:318–321.
7. Licciardi JM, Teller JT, Clark PU (1999) in *Mechanisms of Global Climate Change at Millennial Time Scales: Geophysical Monograph*, eds Clark PU, Webb RS, Keigwin LD (Am Geophys Union, Washington, DC), Vol 112, pp 177–201.

8. Clark PU, Marshall SJ, Clarke GKC, Hostetler SW, Licciardi JM, Teller JT (2001) *Science* 293:283–287.
9. Rodrigues CG, Vilks G (1994) *Quaternary Sci Rev* 13:923–944.
10. Keigwin LD, Jones GA (1995) *Paleoceanography* 10:973–985.
11. deVernal A, Hillaire-Marcel C, Bilodeau G (1996) *Nature* 381:774–777.
12. Teller JT, Boyd M, Yang Z, Kor PSG, Fard AM (2005) *Quaternary Sci Rev* 24:1890–1905.
13. Lowell TV, Fisher TG, Comer GC, Hajdas I, Waterson N, Glover K, Loope HM, Schaefer JM, Rinterknecht V, Broecker W, *et al.* (2005) *Eos* 86:365–373.
14. Tarasov L, Peltier WR (2005) *Nature* 435:662–665.
15. Meybeck M (1987) *Am J Sci* 287:401–428.
16. Barton KE, Howell DG, Vigil JF (2003) Geologic Investigations Series I-2781 (US Geological Survey, Washington, DC).
17. Delaney ML, Bé AWH, Boyle EA (1985) *Geochim Cosmochim Acta* 49:1327–1341.
18. Lea DW, Mashiotta TA, Spero HJ (1999) *Geochim Cosmochim Acta* 63:2369–2379.
19. Yang C, Telmer K, Veizer J (1996) *Geochim Cosmochim Acta* 60:851–866.
20. Mott RJ, Grant DR, Stea R, Occhietti S (1986) *Nature* 323:247–250.
21. Swarzenski PW, Porcelli D, Anderson PS, Smoak JM (2003) in *Uranium-Series Geochemistry: Reviews in Mineralogy and Geochemistry*, eds Bourdon B, Henderson GM, Lundstrom CC, Turner SP (Mineralogical Soc of America, Chantilly, VA), Vol 52, pp 577–606.
22. Russell AD, Emerson SR, Nelson BK, Erez J, Lea DW (1994) *Geochim Cosmochim Acta* 58:671–681.
23. Chabaux F, Riotte J, Dequincey O (2003) in *Uranium-Series Geochemistry: Reviews in Mineralogy and Geochemistry*, eds Bourdon B, Henderson GM, Lundstrom CC, Turner SP (Mineralogical Soc of America, Chantilly, VA), Vol 52, pp 533–576.
24. Russell AD, Hönish B, Spero HJ, Lea DW (2004) *Geochim Cosmochim Acta* 68:4347–4361.
25. Blum JD, Erel Y (1997) *Geochim Cosmochim Acta* 61:3193–3204.
26. Dyke AS (2004) in *Quaternary Glaciations: Extant and Chronology*, eds Ehlers J, Gibbard PL (Elsevier, Amsterdam), Part II, Vol 2b, pp 373–424.
27. Wadleigh MA, Veizer J, Brooks C (1985) *Geochim Cosmochim Acta* 49:1727–1736.
28. Hostetler SW, Bartlein PJ, Clark PU, Small EE, Solomon AM (2000) *Nature* 405:334–337.
29. Remenda VH, Cherry JA, Edwards TWD (1994) *Science* 266:1975–1978.
30. Hillaire-Marcel C, Bilodeau G (2000) *Can J Earth Sci* 37:795–809.
31. Flower BP, Hastings DW, Hill HW, Quinn TM (2004) *Geology* 32:597–600.
32. Smith DG, Fisher TG (1993) *Geology* 21:9–12.
33. Teller JM, Boyd M (2006) *Quaternary Sci Rev* 25:1142–1145.
34. Andrews JT, Dunhill G (2004) *Quaternary Res* 61:14–21.
35. Manabe S, Stouffer RJ (1997) *Paleoceanography* 12:321–336.
36. DeMenocal P, Ortiz J, Guilderson T, Sarnthein M (2000) *Science* 288:2198–2202.
37. Lea DW, Pak DK, Peterson LC, Hughen KA (2003) *Science* 301:1361–1364.
38. Grootes PM, Stuiver M, White JWC, Johnsen S, Jouzel J (1993) *Nature* 369:552–554.
39. Genty D, Blamart D, Ghaleb B, Plagnes V, Causse Ch, Bakalowicz M, Zouari K, Chkir N, Hellstrom J, Wainer K, *et al.* (2006) *Quaternary Sci Rev* 25:2118–2142.
40. Grafenstein VU, Erlenkeuser H, Brauer A, Jouzel J, Johnsen J (1999) *Science* 284:1654–1657.
41. Wang YJ, Cheng H, Edwards RL, An ZS, Wu JY, Shen C-C, Dorale JA (2001) *Science* 294:2345–2348.
42. Blunier T, Brook EJ (2001) *Science* 291:109–112.
43. Haley BA, Klinkhammer GP (2002) *Chem Geol* 185:51–69.
44. Stuiver M, Reimer PJ, Bard E, Beck JW, Burr GS, Hughen KA, Kromer B, McCormac G, van der Plicht J, Spurk M (1998) *Radiocarbon* 40:1041–1083.